2017 International Nuclear Atlantic Conference - INAC 2017
Belo Horizonte, MG, Brazil, October 22-27, 2017
ASSOCIAÇÃO BRASILEIRA DE ENERGIA NUCLEAR - ABEN

Agência Brasileira do ISBN
ISBN 978-85-99141-07-6
9 788599 141076

FIELD DOSE RADIATION DETERMINATION BY ACTIVE LEARNING WITH GAUSSIAN PROCESS FOR AUTONOMOUS ROBOT GUIDING

de Freitas Naiff, Danilo[1], Paulo R. Silveira[2] and Pereira, Claudio M. N. A.[3]

[1]Universidade Federal do Rio de Janeiro - PEN/COPPE/UFRJ
Ilha do Fundo, s/n
21975-970, Rio de Janeiro, RJ
danilonaiff1992@poli.ufrj.br

[2]Universidade Federal do Rio de Janeiro - PEN/COPPE/UFRJ
Ilha do Fundo, s/n
21975-970, Rio de Janeiro, RJ
paulo@lmp.ufrj.br

[3]Instituto de Engenharia Nuclear (IEN/CNEN)
R. Hlio de Almeida, 75 - Ilha do Fundo
21941-614, Rio de Janeiro, RJ
cmnap@ien.gov.br

ABSTRACT

This article proposes an approach for determination of radiation dose profile in a radiation-susceptible environment, aiming to guide an autonomous robot in acting on those environments, reducing the human exposure to dangerous amount of dose. The approach consists of an active learning method based on information entropy reduction, using log-normally warped Gaussian Process (GP) as surrogate model, resulting in non-linear online regression with sequential measurements. Experiments with simulated radiation dose fields of varying complexity were made, and results showed that the approach was effective in reconstruct the field with high accuracy, through relatively few measurements. The technique was also shown some robustness in presence measurement noise, present in real measurements, by assuming Gaussian noise.

1. INTRODUCTION

The reconstruction of radiation dose profile in a spatial environment is a important task given the effects that ionizing radiation has on living organisms. Due to it's importance, an efficient method to determine the measurement points in a environment, and to estimate the full profile given those measurements is of interest, in particular for guiding an autonomous, robotic agent through the environment. The approach used in this work uses a Gaussian Process for both estimation and determination of point measurements by the agent. Previous works using Gaussian Process for active learning and spatial function reconstruction includes [1, 2, 3].

2. METHODOLOGY

2.1. Mathematical Formulation

Let $X \subset \mathbb{R}^2$ be the map containing the dose radiation field, and $g : X \to \mathbb{R}^+$ the unknown dose radiation field function. The objective is to sequentially design a set of n measurement points of X, getting the data $D_n = \{(\mathbf{x}_i, z_i)\}_{i=1:n}$, such as, with those measures, we can estimate a regression function function $g^* : X \to \mathbb{R}^+$ such as g^* is as close as possible from g. We assume further that for each $\mathbf{x}_i$, z_i is a noisy measure of $\mathbf{x}_i$, given by:

$$z_i = g(\mathbf{x}_i)(1 + \epsilon) \tag{1}$$

Here $\epsilon \sim \mathcal{N}(0, \sigma_e^2)$ is a normally distributed random variable.

The regression function g^* is constructed with the use of a Gaussian Process (GP) over the logarithm of g. The Gaussian Process is a regression method that considers a function $f : X \to \mathbb{R}$ to be a random function from the space of functions from X to $\mathbb{R}$, where this random function has the property that, for each finite subset of points $\{\mathbf{x}_i\}_{i=1:m} \subset X$, $\{f(\mathbf{x}_i)\}_{i=1:m}$ follows a multivariate Gaussian distribution [4] Thus, the GP is completely specified by it's mean function $m(\mathbf{x}) := \mathbb{E}[f(\mathbf{x})]$, usually and in this work assumed to be zero, and it's covariance function $k(\mathbf{x}, \mathbf{x}') := cov(f(\mathbf{x}), f(\mathbf{x}^{'}))$, which defines the structure of the GP. In this work, the covariance function used is the isotropic Matrn covariance function with parameter $\nu = 3/2$:

$$k(\mathbf{x}, \mathbf{x}') = C_{3/2}(\mathbf{x}, \mathbf{x}') = \theta_0^2 \exp\left(-\frac{1}{l}\sqrt{3}r\right)\left(1 + \frac{1}{l}\sqrt{3}r\right) \tag{2}$$

Where $r = ||\mathbf{x} - \mathbf{x}'||$. The hyperparameters θ_0^2 and l are called respectively the amplitude parameter and the shape parameter.

With f distributed according to a GP with mean $m(\mathbf{x}) = 0$, and $\mathcal{C}_n = \{(\mathbf{x}_i, y_i)\}_{i=1:n}$ being a previously acquired data, with $y_i = f(\mathbf{x}_i) + \epsilon$, $\epsilon \sim \mathcal{N}(0, \sigma_e^2)$, we have that $f(\mathbf{x})$ is a normally distributed random variable such as $f(\mathbf{x}) \sim p(f(\mathbf{x})|\mathcal{C}_n) = \mathcal{N}(\mu_n(\mathbf{x}), \sigma_n^2(\mathbf{x}))$, where:

$$\begin{aligned} \mu_n(\mathbf{x}) &= \mathbf{k}(\mathbf{x})^T(\mathbf{K} + \sigma_e^2\mathbf{I})^{-1}\mathbf{y} \\ \sigma_n^2(\mathbf{x}) &= k(\mathbf{x}, \mathbf{x}) + \mathbf{k}(\mathbf{x})^T(\mathbf{K} + \sigma_e^2\mathbf{I})^{-1}\mathbf{k}(\mathbf{x}) \end{aligned} \tag{3}$$

Where $\mathbf{k}(\mathbf{x}) := (k(\mathbf{x}_1, \mathbf{x}), \ldots, k(\mathbf{x}_n, \mathbf{x}))^T$ is the covariance vector between $\mathbf{x}$ e $\mathbf{x}_1, \ldots, \mathbf{x}_n$, $\mathbf{y} := (y_1, \ldots, y_n)^T$ is the observed values vector, and $\mathbf{K} = (K_{ij}) \in \mathbb{R}^{n \times n}$, $K_{ij} := k(\mathbf{x}_i, \mathbf{x}_j)$ is the covariance matrix between $\mathbf{x}_1, \ldots, \mathbf{x}_n$.

By letting $f = \log(g)$, and $y_i = \log(z_i) = \log(g(\mathbf{x}_i)(1 + \epsilon)) \approx log(g(\mathbf{x}_i)) + \epsilon$, we can apply the GP over the logarithm of g. This way, given $\mathcal{D}_n$ as defined above, we have that $g(\mathbf{x})$ is a log-normally distributed random variable such as $g(\mathbf{x}) \sim p(g(\mathbf{x})|\mathcal{D}_n) = Lognormal(\mu_n(\mathbf{x}), \sigma_n^2(\mathbf{x}))$, where μ_n and σ_n^2 are as defined above.

The hyperparameters θ_0 and l, collectively called Θ, can be optimized by maximizing the

log-likelihood of $\mathcal{D}_n$ [5]:

$$\begin{aligned}\mathcal{L} = \log(p(\mathcal{D}_n|\Theta)) = &-\frac{1}{2}\log\det(\mathbf{K}+\sigma_e^2\mathbf{I}) - \frac{1}{2}\mathbf{y}^T(\mathbf{K}+\sigma_e^2\mathbf{I})^{-1}\mathbf{y} \\ &-\frac{n}{2}\log(2\pi) - \sum_{i=1}^{n}\log z_i\end{aligned} \tag{4}$$

The regression function $g^*(\mathbf{x})$ of $g(\mathbf{x})$ is given by a point measure of $p(g(\mathbf{x})|\mathcal{D}_n)$. In this work we use the median, minimizing the expected absolute error, so we have that $g^*(\mathbf{x}) = \exp(\mu_n(\mathbf{x}))$.

The GP can also be used to sequentially determine the set of points to be measure. This practice of autonomous determination of learning points is also known as active learning [6]. Given $\mathcal{D}_n$, we want to choose a point $\mathbf{x_{n+1}}$ so the expected data $\mathcal{D}_{n+1} = \mathcal{D}_n \cup \{(\mathbf{x}, y)\}$ can improve our knowledge of g as much as possible. One criteria that can be used is based on a information entropy criterion, in which $\mathbf{x}_{n+1}$ is chosen so that $g(\mathbf{x}_{n+1})$ has the maximal differential entropy [1]. Since $g(\mathbf{x})$ is log-normally distributed, this means that we want to maximize $h(g(\mathbf{x})) = \mu_n(\mathbf{x}) + \frac{1}{2}\log(2\pi e\sigma_n^2(\mathbf{x}))$, then getting $\mathbf{x}_{n+1}$ as $\arg\max_x \alpha_n(\mathbf{x}) := h(g(\mathbf{x}))$. Thus function $h(g(\mathbf{x}))$ has to be optimized for getting $\mathbf{x}_{n+1}$. The function α_n is also called the acquisition function.

2.2. Algorithm

Using the above method, it is designed algorithm for autonomous determination of point measurements of dose radiation in a known map, with the objective of reconstructing the field of dose radiation. In this algorithm we manually set the hyperparameters optimization frequency N_{opt}, the initial hyperparameters θ_0 and l for the first N_{opt} measurements, the initial position of the agent $\mathbf{x}_0$, and a stopping criterion, in this work being a total number N of measurements. The pseudocode of the algorithm is shown in figure 1.

GP ← initialize GP
$\mathbf{x} \leftarrow \mathbf{x}_0$
z ← *MEASURE_RADIATION()*
GP ← *ADD_DATA(GP,*{$\mathbf{x}$,log *z*}*)*
counter ← *1*
while *counter* ≤ $N - 1$ **do**
    α_n ← *GET_AQUISITION_FUNCTION(GP,x)*
    $\mathbf{x}$ ← *OPTIMIZE*(α_n*)*
    y ← *MEASURE_RADIATION*($\mathbf{x}$*)*
    GP.ADD_DATA({$\mathbf{x}$,*y*}*)*
    counter ← *counter* + 1
    if $i \bmod N_{opt} = 0$ **then** *GP* ← *UPDATE_PARAMETERS(GP)*
g^* ← *GET_MEDIAN(GP)*
return g^*

Figure 1: Algorithm for autonomous determination of point measurements

2.3. Simulations

The active regression method was studied in two hypothetical dose functions g_a and g_b in a $20m \times 20m$ room, which were constructed as sums of basis functions of form $\phi(x, y; x_0, y_0, h, K) = K/((x-x_0)^2+(y-y_0)^2+h^2)$, so that $g_p(\mathbf{x}) = g(x, y) = \sum_i \phi_p^i(x, y)$, with p denoting either the index a or b. The function g_a is composed of 4 roughly equally spaced and equally shaped basis functions, while g_b is composed of 12 unevenly shaped and spaced basis functions, giving it a much higher complexity than g_a. The plot of both functions are shown in figure 2.

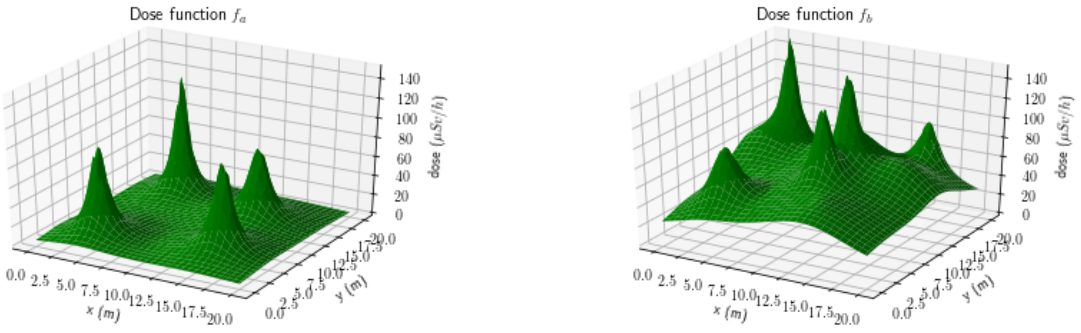

(a) 4 basis functions

(b) 12 basis functions

Figure 2: Dose functions used in simulations

For each of the dose radiation functions, two scenarios are considered, one where there is no measurement error, (σ_e equals 0), and a 1% measurement error (σ_e equals 0.01). The agent initial position x_0 is set to $10m \times 10m$, so the first measurement is made in the middle of the map, θ_0 and l to 1 and $1m$ respectively, N_{opt} to 10, and N to 100. The acquisition function was optimized using a differential evolution algorithm. Given the stochastic nature of measurements (where σ_e is not 0), and of the optimization algorithm, three trials were made for each of the cases above.

3. RESULTS

3.1. Four Basis Functions Field Case

3.1.1. Without measurement error

In scenario assuming no measurement error, the dose field reconstruction of g_a was highly accurate, with the three trials finding the four peaks within 75 evaluations, as shown in the the error figure 3. The final mean relative error of the three trials after 100 evaluations were around 1%.

The final field estimation for one of the trials is shown in figure 4, where is seen that the estimation was done closely resembling the original function. The evaluation points are shown in figure 5, where clusters of evaluation points around the peaks are seen.

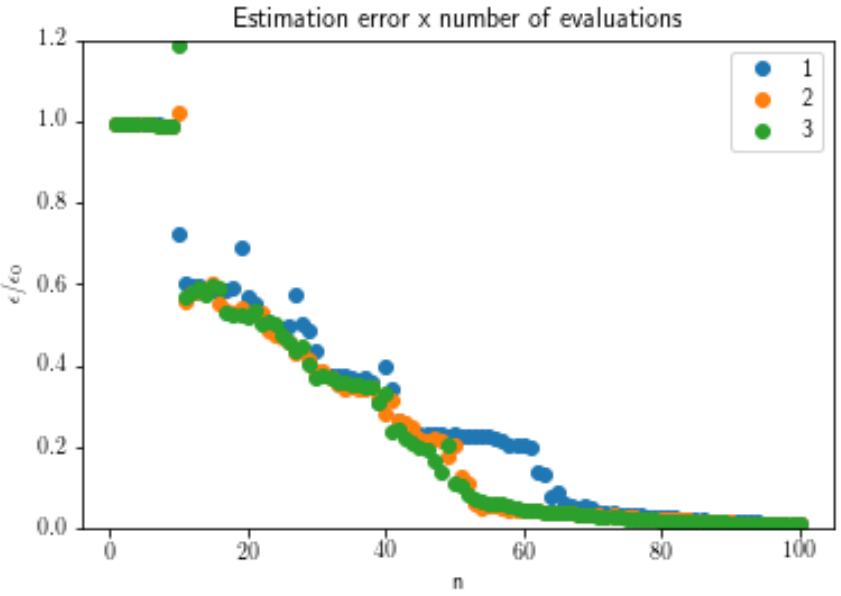

Figure 3: Evolution of the estimation mean relative error of g_a in the no measurement error case.

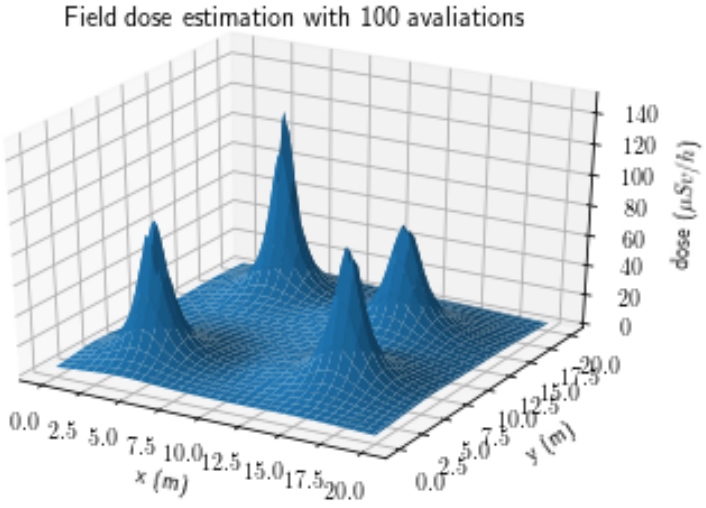

Figure 4: Final estimation of g_a in the no measurement error case.

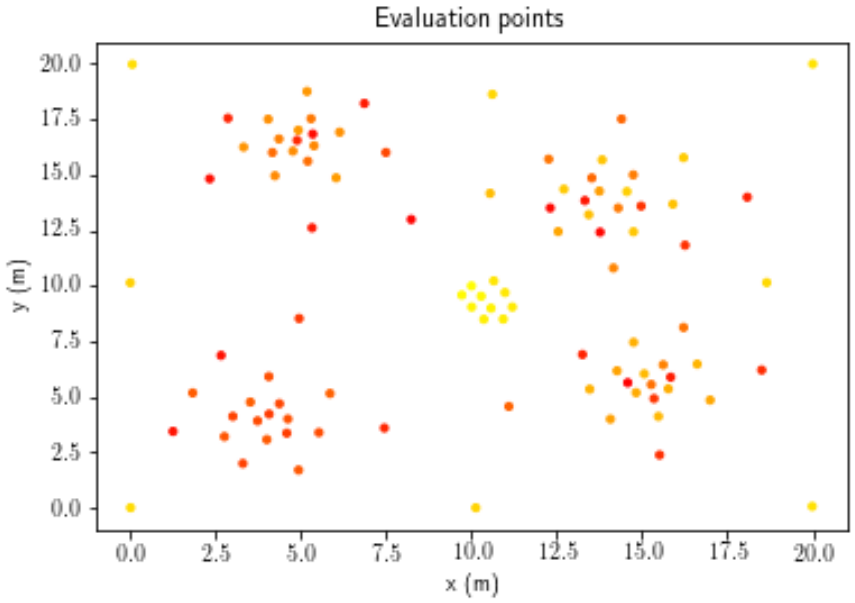

Figure 5: Evaluation points for g_a in the no measurement error case. Yellower points are early evaluations, while redder points are later evaluations.

3.1.2. With measurement error

In the scenario assuming a 1% measurement error, the reconstruction showed problems, with only one of the three trials the agent finding all of the four peaks after 100 evaluations, with the other two trials finding only three of the peaks, as shown in figure 6.

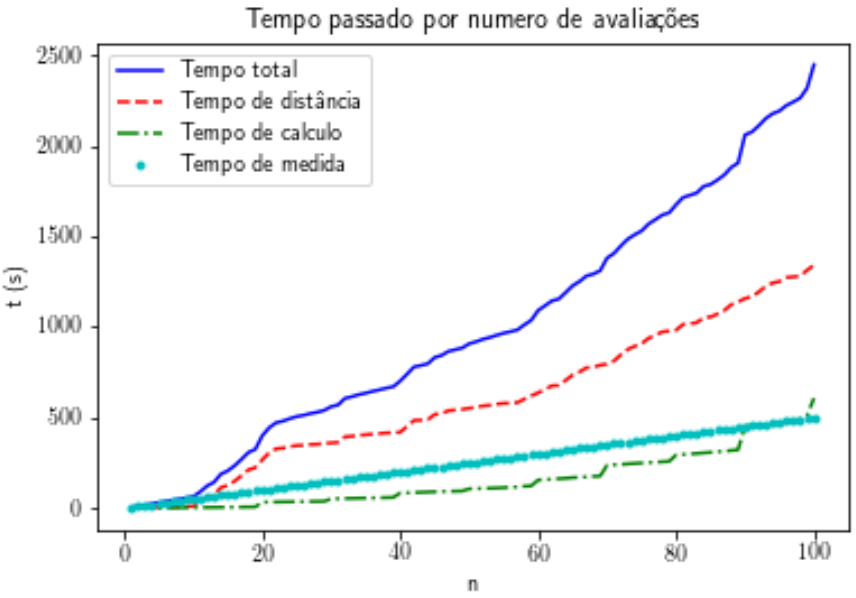

Figure 6: Evolution of the estimation error of g_a in the 1% measurement error case.

The final field found in one of the failed trials is shown in figure 7, The evaluation points order in figure 8 shows that there was indeed a region unexplored in the algorithm, where the remaining peak was located.

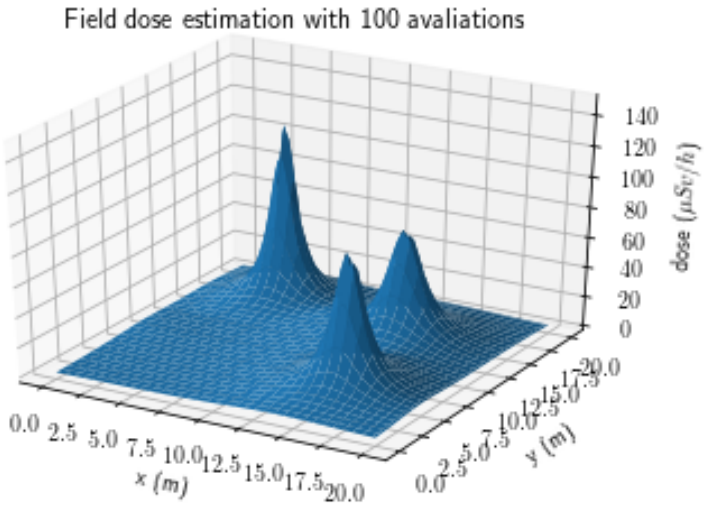

Figure 7: Final estimation of g_a in the 1% measurement error case.

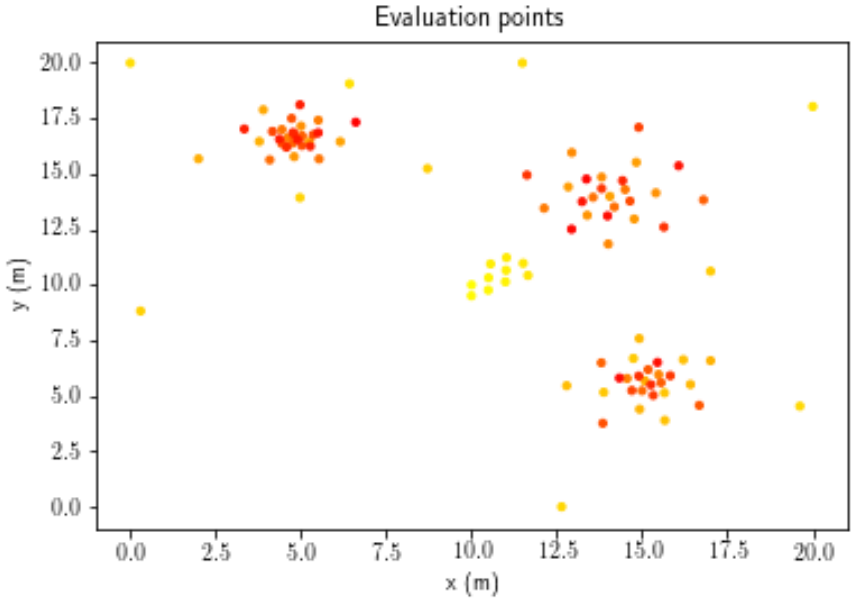

Figure 8: Evaluation points for g_a in the 1% measurement error case

3.2. Twelve Basis Functions Field Case

3.2.1. Without measurement error

In scenario assuming no measurement error, even thought the g_b function is more complex than the previous one, the reconstruction was still accurate, as shown in figure 9, with a final mean relative error of the three trials after 100 evaluations were around 2.5%.

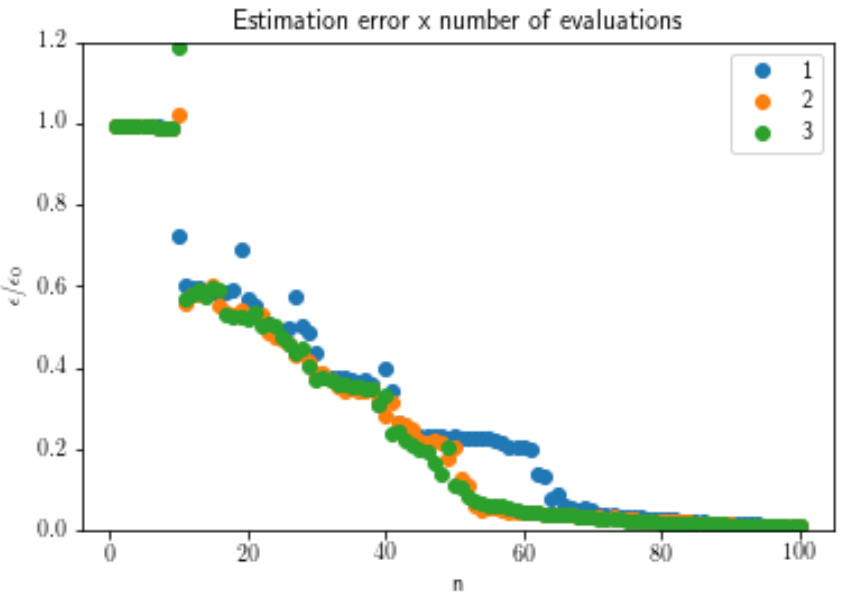

Figure 9: Evolution of the estimation error for g_b in the no measurement error case

The final field estimation for one of the trials shown in figure 10 resembles closely the original field. The evaluation points showed in figure 11 shows disperse evaluation points, which may be due the higher complexity of the measured function, preventing formation of clusters of measurements.

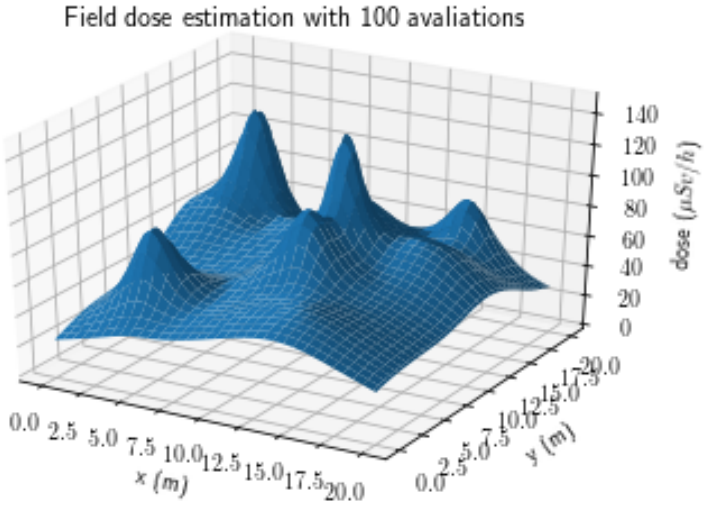

Figure 10: Final estimation of g_b in the no measurement error case

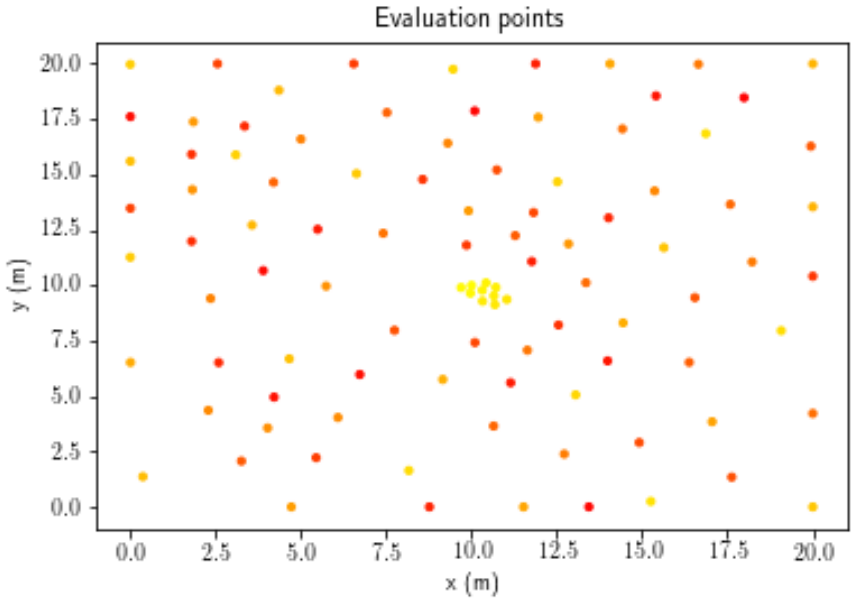

Figure 11: Evaluation points for the g_b function measurement, showing more disperse evaluation points

3.2.2. With measurement error

In the scenario assuming a 1% measurement error, although the reconstruction was flawed, it was more accurate than in the g_a function case, as shown in figure 12, resulting in a final estimation error around 5%. The final plot of one of the trials is shown in figure

13. This higher accuracy, compared to the g_a case, be due to the scattered points of measurements, which makes it harder to miss larger peaks.

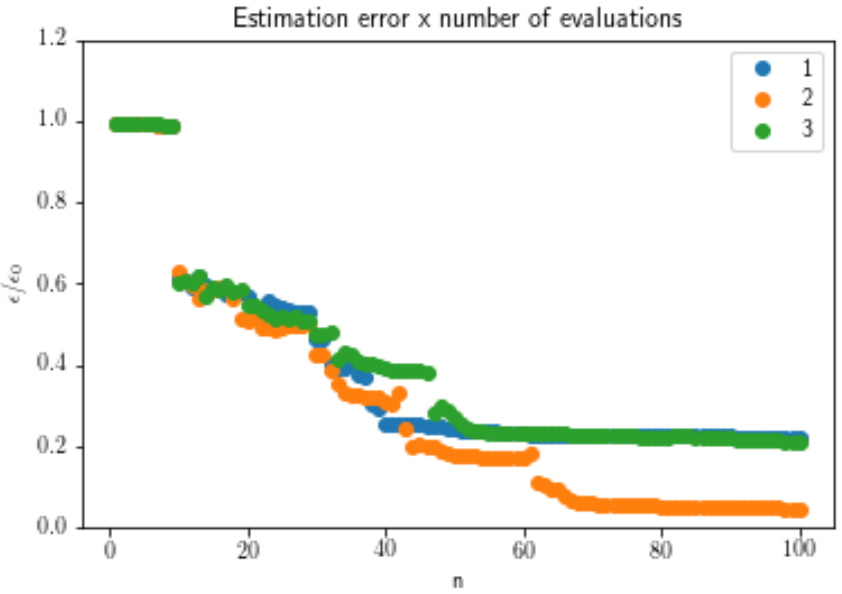

Figure 12: Evolution of the estimation error for g_b in the 1% measurement error case

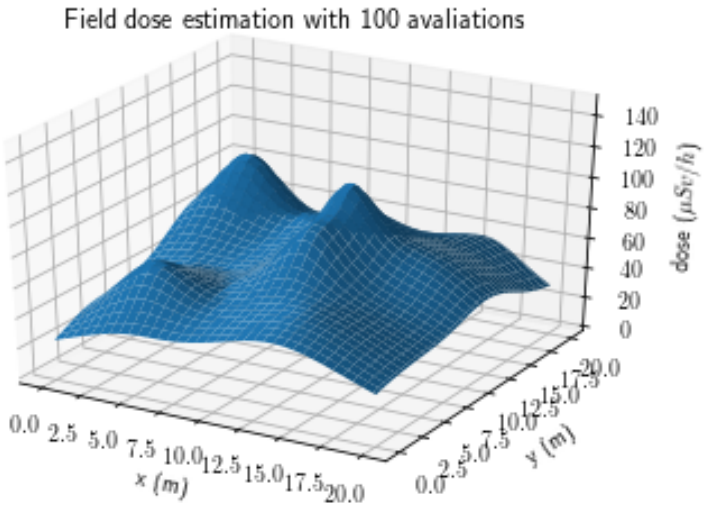

Figure 13: Final estimation for g_b in the 1% measurement error case

4. CONCLUSIONS

The method for autonomous determination of point measurements and regression outlined above fared well in both simulated situations, specially with the no measurement error

assumption. Further tests with actual physical agents remains to be done to see how the method fares in a real setting.

ACKNOWLEDGMENTS

This work has been possible with the support of Laboratório de Monitoramento de Process (LMP) - COPPE/UFRJ.

REFERENCES

1. A. Krause, A. Singh, C. Guestrin, "Near-optimal sensor placements in Gaussian processes: Theory, efficient algorithms and empirical studies", *J. Machine Learning Research*, **9**, pp. 235-284, (2008).
2. A. Krause and C. Guestrin, "Nonmyopic active learning of Gaussian processes: an exploration-exploitation approach", *ICML '07: Proc. of the 24th int. conf. on Machine learning*, pp. 449-456, (2007).
3. Dongbing Gu and Huosheng Hu, "Active learning of Gaussian processes for spatial functions in mobile sensor networks", *Preprints of the 18th IFAC World Congress*, Milano (Italy), August 28 - September 2, (2011).
4. C. E. Rasmussen and C. K. I. Williams, *Gaussian Processes for Machine Learning*, The MIT Press, (2006).
5. E. Snelson, C. E. Rasmussen, Z. Ghahramani, "Warped Gaussian Processes", *Advances in Neural Information Processing Systems*, (2006).
6. B. Settles, "Active Learning Literature Survey",*Computer Sciences Technical Report*, 1648, University of Winconsin-Madison, (2010).